

Type II Cadherins Guide Assembly of a Direction-Selective Retinal Circuit

Xin Duan,^{1,2,4} Arjun Krishnaswamy,^{1,2,4} Irina De la Huerta,^{1,2,3} and Joshua R. Sanes^{1,2,*}

¹Center for Brain Science, Harvard University, Cambridge, MA 02138, USA

²Department of Molecular and Cellular Biology, Harvard University, Cambridge, MA 02138, USA

³Present address: Department of Ophthalmology, University of California, San Francisco, San Francisco, CA 94143, USA

⁴Co-first author

*Correspondence: sanesj@mcb.harvard.edu

<http://dx.doi.org/10.1016/j.cell.2014.06.047>

SUMMARY

Complex retinal circuits process visual information and deliver it to the brain. Few molecular determinants of synaptic specificity in this system are known. Using genetic and optogenetic methods, we identified two types of bipolar interneurons that convey visual input from photoreceptors to a circuit that computes the direction in which objects are moving. We then sought recognition molecules that promote selective connections of these cells with previously characterized components of the circuit. We found that the type II cadherins, *cdh8* and *cdh9*, are each expressed selectively by one of the two bipolar cell types. Using loss- and gain-of-function methods, we showed that they are critical determinants of connectivity in this circuit and that perturbation of their expression leads to distinct defects in visually evoked responses. Our results reveal cellular components of a retinal circuit and demonstrate roles of type II cadherins in synaptic choice and circuit function.

INTRODUCTION

Complex neural circuits underlie mental activities, and defects in circuit assembly likely underlie some behavioral disorders. Elucidating the mechanisms that instruct circuit assembly is therefore a main item in the agenda of developmental neurobiology. An increasingly feasible program for accomplishing this goal involves (1) categorizing the cell types that comprise the neuronal ensemble, (2) gaining genetic access to them, so they can be marked and manipulated, (3) mapping their connectivity, (4) identifying candidate mediators of specific connectivity among them, and (5) using loss- and gain-of-function methods to assess roles of the candidates on circuit structure and function.

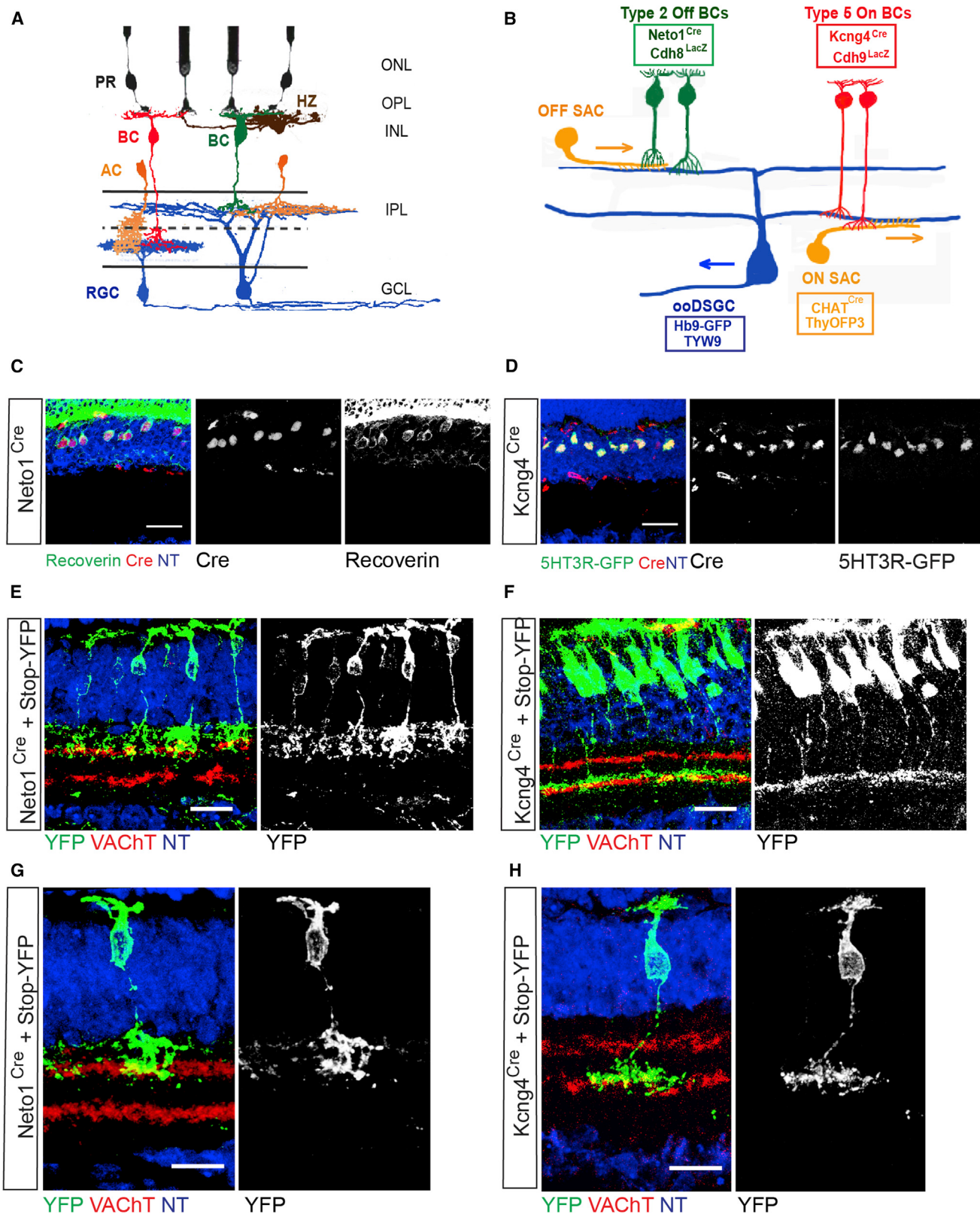
The mouse retina has emerged as an excellent model system for implementing this program (Masland, 2012; Sanes and Zipursky, 2010). It contains ~100 neuronal types and is therefore about as complex as other brain areas, but it has several advantages that facilitate analysis, including an orderly arrangement of

its cells and synapses, accessibility to study, and an impressive background of information about its structure and function. Its neurons are arranged in three cellular (nuclear) layers separated by two synaptic (plexiform) layers (Figure 1A). Photoreceptors synapse on bipolar and horizontal interneurons in the outer plexiform layer. Bipolar cells (BCs) carry visual information to the inner plexiform layer (IPL) where the information is processed by amacrine cells and retinal ganglion cells (RGCs); the RGCs carry information to the brain. The IPL is divided into approximately ten sublaminae, with processes of most cell types restricted to just one or a few of them. Thus, the laminar restriction of axonal and dendritic processes is a major determinant of specific connectivity in the IPL.

As a consequence of laminar specificity, each of ~30 RGC subtypes receives inputs from a restricted subset of interneurons, which endows it with the ability to respond preferentially to particular features in the visual world, such as motion or color contrast (Gollisch and Meister, 2010). Among the most intensively studied RGCs are those that respond selectively to motion in particular directions. Eight types of direction-selective ganglion cells (DSGCs) have been described, including four ON-OFF DSGCs (ooDSGCs) that respond to both increases and decreases in intensity of illumination (Vaney et al., 2012) (Figure 1B).

Each of the four subsets of ooDSGCs responds preferentially to motion in one of the cardinal directions—nasal, temporal, dorsal, and ventral (Oyster and Barlow, 1967). Their direction selectivity arises primarily from inhibitory interneurons called starburst amacrine cells (SACs). SAC dendrites are themselves direction-selective, releasing GABA onto ooDSGCs when an object moves from proximal to distal along the dendrite. Thus, the preferred direction of each ooDSGC is opposite to that of the innervating SAC dendrites (Vaney et al., 2012). The SACs and ooDSGCs, in turn, receive their visual input through excitatory synapses made by BCs. Twelve BC types have been identified in mouse, which can be classified into ON and OFF groups (Wässle et al., 2009); they excite their targets when illumination increases (ON responses) or decreases (OFF responses). ON and OFF BCs stratify in inner and outer portions of the IPL, respectively (Famiglietti and Kolb, 1976). As ON-OFF cells, ooDSGCs have bistratified dendrites and are innervated by both ON and OFF BCs.

Structural and functional information about ooDSGCs and SACs provides a strong foundation for molecular and developmental studies. Each of the four ooDSGC subtypes is



(legend on next page)

molecularly distinct (Huberman et al., 2009; Kim et al., 2010) as are the ON and OFF SACs (Sun et al., 2013). Molecular and functional distinctions among ooDSGC subtypes are established prior to and independent of visual experience (De la Huerta et al., 2012; Kim et al., 2010; Wei and Feller, 2011). Several genes responsible for patterning the somata and dendrites of SACs have been identified (Kay et al., 2012; Lefebvre et al., 2012; Sun et al., 2013), but the BC subtypes that provide input to SACs and ooDSGCs remain poorly defined and for no cells in the circuit have molecules been identified that target their processes to specific sublamininae.

We address these issues here. First, we used molecular markers to gain genetic access to Type 2 OFF and Type 5 ON BCs (BC2s and BC5s) and showed that they provide direct input to ooDSGCs and SACs. Second, we showed that two type II cadherins, *cdh8* and *cdh9*, are selectively expressed by BC2s and BC5s, respectively. Third, we used loss- and gain-of-function strategies to show that *Cdh8* and *Cdh9* play instructive roles in targeting BC2s and BC5s to appropriate sublamininae. Finally, we show that *Cdh8* and *Cdh9* are required for connections from BCs to their targets and for visually-evoked responses of ooDSGCs.

The cadherins are a major family of recognition molecules. Among the >100 members of the cadherin superfamily, the best studied are the classical (types I and II) cadherins, a set of ~20 closely related transmembrane homophilic adhesion molecules. Classical cadherins are expressed in complex, combinatorial patterns throughout the central nervous system (CNS) and have been implicated in several aspects of neural development (see Discussion). Their elaborate patterns of expression have led to the hypothesis that they also mediate target recognition within or among areas. Our results provide direct support for this hypothesis.

RESULTS

Genetic Access to Elements of an ON-OFF Direction-Selective Circuit

In previous studies, we and others characterized transgenic lines that express fluorescent proteins or Cre recombinase in several subsets of ooDSGCs and SACs (Huberman et al., 2009; Kim et al., 2010; Kay et al., 2011a; Rossi et al., 2011; Trenholm et al., 2011). To begin this study, we sought markers for BCs that provide visual input to ooDSGCs and SACs, based on laminar position of their axonal arbors. These include BC2s and BC5s (Helmstaedter et al., 2013; Wässle et al., 2009). We identified candidate markers from published databases (Kay et al., 2012; Kim et al., 2008) and screened them by *in situ* hybrid-

ization. Consistent with previous results (Chow et al., 2004; Siegert et al., 2009), *neto1* and *kcnq4* were selectively expressed by BC2s and BC5s (data not shown).

We then generated “knock-in” mouse lines in which Cre recombinase is inserted at the translational start site of the *neto1* and *kcnq4* genes (Figures S1A and S1B available online). Cre was expressed in subsets of BCs in these lines as judged by immunostaining for Cre or mating to Cre-dependent reporters (Buffelli et al., 2003; Madisen et al., 2012) (Figures 1C–1F and data not shown). Some RGCs and amacrine cells were also Cre-positive. Several lines of evidence confirmed that the labeled BCs were BC2s in the *Neto1*^{Cre} line and BC5s in the *Kcnq4*^{Cre} line. First, *Neto1*^{Cre}-positive BCs expressed recoverin (Figure 1C), a marker of BC2s in the INL (Haverkamp et al., 2003). Second, we mated *Kcnq4*^{Cre} mice to a 5HT3R-GFP transgenic line that specifically marks BC5s (Haverkamp et al., 2009). Cre-positive BCs were uniformly GFP-positive in double transgenic offspring (Figure 1D). Third, cells labeled by introduction of Cre-dependent reporter plasmids into *Neto1*^{Cre} line and *Kcnq4*^{Cre} mice resembled BC2s and BC5s characterized previously (Wässle et al., 2009) (Figures 1E–1H). Fourth, consistent with previous analysis (Wässle et al., 2009), *Neto1*⁺ and *Kcnq4*⁺ BCs account for 8% and 14% of total BCs (*Chx10*⁺ cells) in the adult retina (Figure S1C). Thus, the *Neto1*^{Cre} and *Kcnq4*^{Cre} lines provide genetic access to BC2s and BC5s, respectively.

Next, we used an optogenetic method to ask whether BC2s and BC5s synapse on SACs or ooDSGCs. *Neto1*^{Cre} and *Kcnq4*^{Cre} mice were bred to transgenic lines in which SACs or ooDSGCs were marked with fluorescent proteins (Figure 1B). Channelrhodopsin (ChR2) was introduced into the BCs using either a transgenic line (Madisen et al., 2012) or an adeno-associated viral vector (AAV) in which expression is Cre-dependent (Cardin et al., 2009). Marked SACs or ooDSGCs were targeted for recording in explants and BCs were stimulated individually using two-photon illumination (Andrasfalvy et al., 2010; Rickgauer and Tank, 2009) to avoid activating photoreceptors (Figure S2). By probing all BCs near a targeted ooDSGC or SAC (Figures S2A and S2B), we could compute their convergence in the circuit.

Stimulation of either BC2s or BC5s evoked currents in ooDSGCs (Figures 2A and 2B). The short latency of the responses (<5 ms) demonstrated that the connections were monosynaptic. BC-evoked currents had reversal potentials near 0 mV and were blocked by NBQX (40 μM), indicating glutamatergic transmission (Figures 2A, 2B, 2E, and S2D). BC5s, but not BC2s, also made excitatory synapses on ON SACs, consistent with their stratification patterns (Figures 2C, 2E, and S2D); we were unable to target

Figure 1. Molecular Characterization of a Direction-Selective Circuit

- (A) Sketch showing retinal cell types and layers. PR, photoreceptor; HZ, horizontal cell; BC, bipolar cell; AC, amacrine cell; RGC, retinal ganglion cell; ONL, outer nuclear layer; INL, inner nuclear layer; GCL, ganglion cell layer; OPL, outer plexiform layer; IPL, inner plexiform layer.
 - (B) Main cell types of the ON-OFF direction-selective circuit. Arrows show preferred direction of motion in starburst amacrine cell (SAC) dendrites (orange arrows) and ON-OFF direction-selective RGC (ooDSGC; blue arrow). Mouse lines used to mark and manipulate each cell type are indicated. Only the synapse-forming SAC dendrites are drawn for clarity.
 - (C and D) Immunostaining for Cre in *Neto1*^{Cre} and *Kcnq4*^{Cre} lines. *Neto1* is coexpressed with the Type 2 OFF BC (BC2) marker, recoverin. *Kcnq4* is coexpressed with GFP in the Type 5 ON BC (BC5) specific transgenic line, 5HT3R-GFP. Scale bars represent 20 μm.
 - (E and F) BCs labeled in *Neto1*^{Cre}; stop-YFP (BC2s, E) and *Kcnq4*^{Cre}; stop-YFP (BC5s, F) retinas. Scale bars represent 15 μm.
 - (G and H) Single BC labeled by infection with AAV expressing Cre-dependent membrane-YFP in *Neto1*^{Cre} (BC2, G) and *Kcnq4*^{Cre} (BC5, H) retina. Sections in (E–H) counterstained with Neurotrace (blue) and antibodies to vesicular acetylcholine transporter (VACHT; red). Scale bars represent 8 μm.
- See also Figure S1 and Tables S1 and S2.

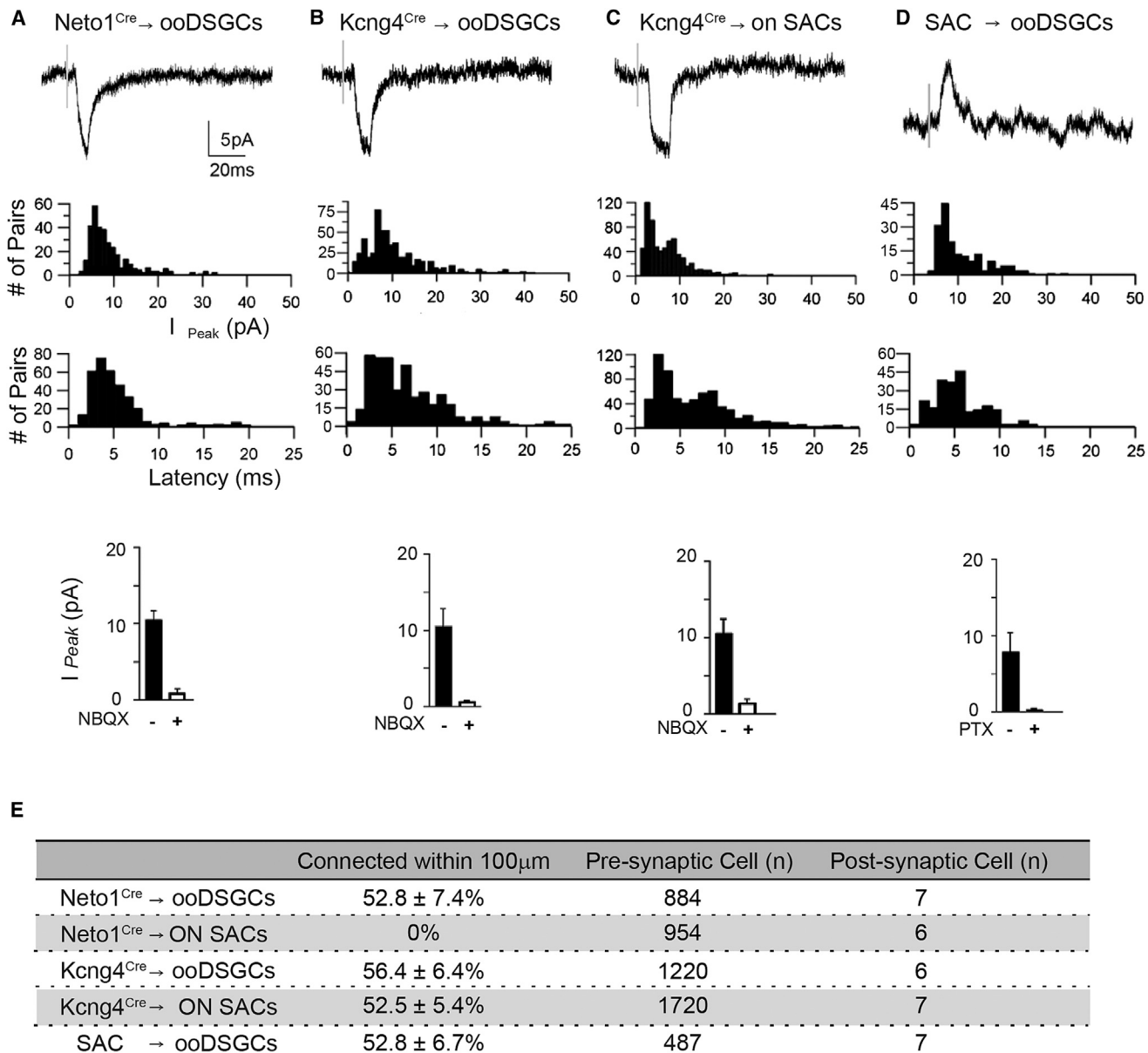


Figure 2. Synaptic Targets of OFF BC2s and ON BC5s

(A–C) Whole-cell currents recorded from ooDSGCs and SACs following optogenetic stimulation of BC2s or BC5s (holding potential $V_h = -60$ mV). Graphs show distribution of peak amplitudes and latencies of currents. Inward currents evoked in ooDSGCs and SACs by stimulation of BCs were blocked by the glutamatergic antagonist, NBQX (40 μM, bottom row; n = 5–7).

(D) Whole-cell currents (top) recorded from ooDSGCs following optogenetic stimulation of SACs ($V_h = -10$ mV). Graphs show peak amplitudes and latencies of currents. Outward currents evoked in ooDSGCs by stimulation of SACs are blocked by the GABAergic antagonist, picrotoxin (PTX, 100 μM, bottom row, n = 5).

(E) Percentages of pre-post synaptic connectivity determined as shown in (A)–(D). No connectivity from BC2s (Neto1⁺ BCs) to ON SACs was detected. See also Figure S2.

OFF SACs in the INL for recording, but recent ultrastructural results suggest that they are innervated by BC2s (Helmstaedter et al., 2013). SACs, in turn, formed inhibitory GABAergic synapses and excitatory cholinergic synapses on ooDSGCs (Figures 2D, 2E, and S2E), consistent with previous results (Vaney et al., 2012). Thus, our optogenetic tests revealed two components of the direction-selective circuit, BC2s and BC5s.

Cdh8 and Cdh9 Are Expressed by BC2s and BC5s

We next sought synaptic recognition molecules that might promote connectivity of BC2s and BC5s with SACs or ooDSGCs. We were particularly interested in the classical (type I and type II) cadherins based on previous findings that some members of this family are expressed by neuronal subsets in mouse and chick retina (Honjo et al., 2000; Kay et al., 2011a; Yamagata et al.,

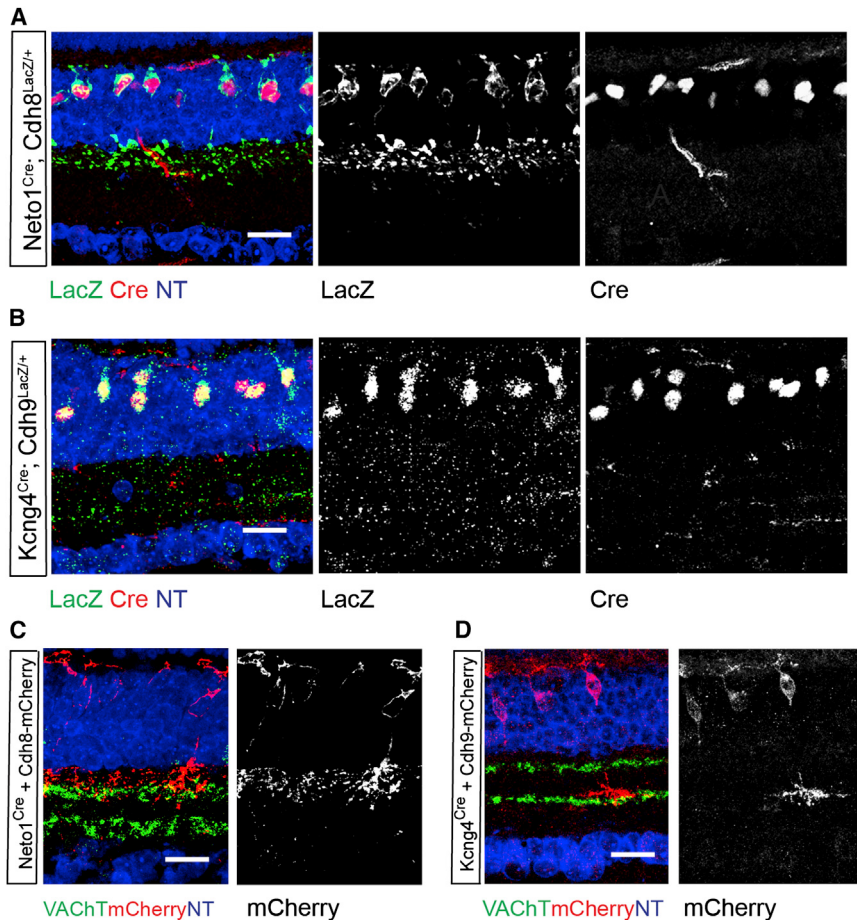


Figure 3. Expression of Cdh8 and Cdh9 in BC2s and BC5s

(A and B) Immunostaining for LacZ and Cre in Neto1^{Cre/+}; Cdh8^{LacZ/+} (A) and Kcng4^{Cre/+}; Cdh9^{LacZ/+} (B) mice. Scale bars represent 10 μm. (C and D) Localization of Cdh8-mCherry in BC2s (Neto1^{Cre/+} mice; C) and of Cdh9-mCherry in BC5s (Kcng4^{Cre/+} mice, D). Scale bars represent 10 μm. See also Figures S3 and S4 and Tables S3 and S4.

tochemical analysis, so we generated Cdh8- and Cdh9-mCherry fusion proteins, showed that they were biologically active (see below), and expressed them in BCs by electroporation of Cre-dependent vectors in Neto1^{Cre} or Kcng4^{Cre} mice. Whereas membrane-bound fluorescent proteins were diffusely distributed throughout the cells (Figures 1G and 1H), the cadherins were concentrated in the axonal and dendritic arbors of the BCs (Figures 3C and 3D). Thus, the localization of these cadherins is consistent with the possibility that they are involved in synapse formation.

Cdh8 and Cdh9 Are Required for Laminar Restriction of BC Arbors

To ask whether Cdh8 is required for the development of BC2s, we compared the morphology of labeled cells in *cdh8* mutants and controls. Sections were double-stained with antibodies to the vesicular acetylcholine transporter (VACHT) to mark SAC dendrites.

Deletion of *cdh8* had no detectable effect on the number of BC2s, the positions of their somata, or the extension of their axons into the IPL. However, instead of being confined to a single sublamina, axonal arbors were evenly distributed between the two sublaminae—one in the position of control BC2s and the other overlapping the ON SAC dendrites on which BC5s synapse (Figures 4A, 4B, and 4D). This alteration might reflect formation of bistratified arbors by some mutant BC2s or displacement of arbors of a subset of mutant BCs. To distinguish these possibilities, we used AAV expressing Cre-dependent YFP to label BCs sparsely. Individual BC2s were not bistratified in the absence of *cdh8*; rather, ~50% bore arbors similar to those in controls, while the others bore monostratified but displaced arbors (Figure 4I). We also considered the possibility that deletion of *cdh8* transformed some BC2s into another BC subtype. Evidence against such transformation is that mutant cells continued to express two specific markers of BC2s—*cdh8*, as judged by expression of *lacZ* from the *cdh8* locus in Cdh8^{LacZ/LacZ} mice and *neto1*, as judged by expression of *cre* from the *neto1* locus in Neto1^{Cre/+} mice (Figures 4B and 4L–4S). Thus, *cdh8* selectively affects placement of BC2 arbors rather than globally affecting BC identity.

We used a similar strategy to seek a role for Cdh9 in arborization of BC5s. Paralleling results from Cdh8-deficient BC2s,

2006). We used *in situ* hybridization to survey cadherin expression in the retina at P7 and P14, times that span the interval during which BCs form synapses (Morgan et al., 2006). Several cadherins were expressed by neuronal subsets during this period (Figure S3). Among them, two type II cadherins, *cdh8* and *cdh9* (Figures S3L and S3N), were selectively expressed by subsets of cells identifiable as BCs by their position in the outer portion of the INL. Levels of *cdh8* mRNA decreased and levels of *cdh9* increased between P7 and P14 but both were expressed throughout the period of BC synaptogenesis (Figure S3).

Double-label *in situ* hybridization suggested that the Cdh8⁺ and Cdh9⁺ BCs were BC2 and BC5, respectively (Figure S4D and data not shown). To test this idea, and to investigate roles of Cdh8 and Cdh9, we obtained *cdh8* null mutant mice (Suzuki et al., 2007) and generated *cdh9* null mutant mice (Figures S4A–S4C); *lacZ* was inserted into the locus in both alleles (Cdh8^{LacZ} and Cdh9^{LacZ}), providing a reporter. We mated these mice to the Neto1^{Cre} and Kcng4^{Cre} lines described above and stained sections with antibodies to Cre and LacZ. Immunoreactivity for LacZ and Cre overlapped in Neto1^{Cre/+}; Cdh8^{LacZ/+} and Kcng4^{Cre/+}; Cdh9^{LacZ/+} mice (Figures 3A and 3B). Thus, *cdh8* and *cdh9* are selectively expressed by BC2s and BC5s.

We next asked where Cdh8 and Cdh9 proteins are localized within BCs. Available antibodies are unsuitable for immunohis-

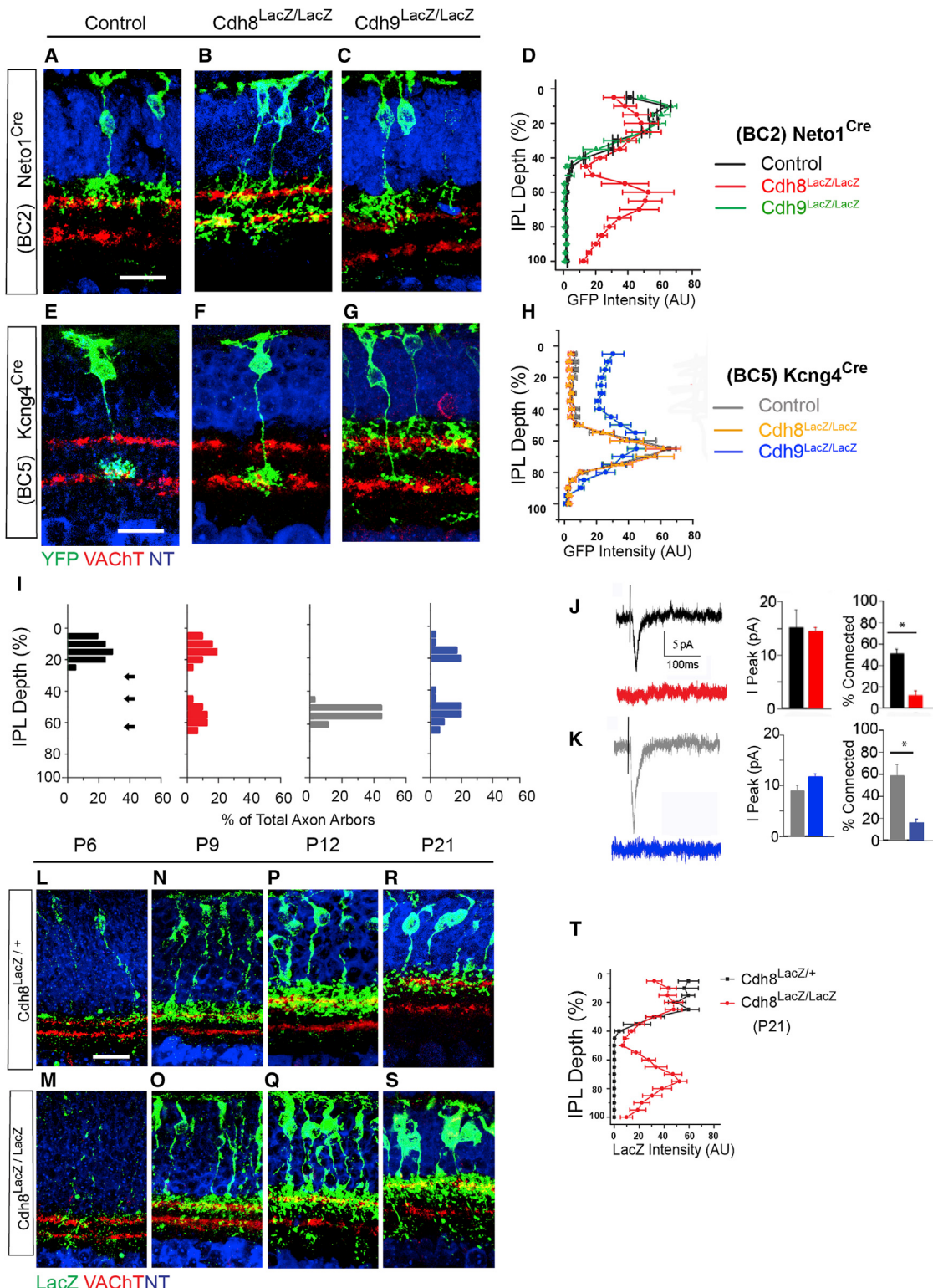


Figure 4. Effects of Deleting *cdh8* and *cdh9* on Axonal Arbors of BC2s and BC5s and the Role of *cdh8* in BC2s during Development
 (A–D) BC2s labeled in Neto1^{Cre/+} (A), Neto1^{Cre/+}; Cdh8^{LacZ/LacZ} (B) or Neto1^{Cre/+}; Cdh9^{LacZ/LacZ} mice (C). (D) Mean intensity (\pm SEM) of YFP label across the IPL from images such as those shown in (A–C). n = 33 (A), n = 35 (B), and n = 40 (C).

(legend continued on next page)

deletion of *cdh9* (*Cdh9*^{LacZ/LacZ}; *Kcng4*^{Cre/+};stop-YFP mice) had no detectable effect on the number, somata or identity of BC5s, but led to displacement of arbors of one-third of the labeled cells. In this case, arbors were displaced to the outer half of the IPL, including to the sublamina in which BC2s arborize (Figures 4E and 4G–4I).

We assayed the specificity of these defects in two ways. First, we asked whether loss of *Cdh9* affected BC2s or loss of *Cdh8* affected BC5s. To this end, we generated *Cdh9*^{LacZ/LacZ}; *Neto1*^{Cre/+};stop-YFP and *Cdh8*^{LacZ/LacZ}; *Kcng4*^{Cre/+};stop-YFP mice. BC arbors in these mice were not detectably different from those in controls (Figures 4C, 4D, 4F, and 4H). Second, we asked whether loss of *Cdh8* or *Cdh9* affected arbors of other neuronal subtypes, including ooDSGCs, SACs, rod BCs, type 3a OFF BCs, tyrosine-hydroxylase-positive wide-field amacrine cells, and VGlut3-positive narrow-field amacrine cells. In no case did arbors in the two mutants differ detectably from those in controls (Figure S5 and data not shown).

Cdh8 and Cdh9 Are Required for Functional Connectivity from BCs to ooDSGCs

To assess the effects of *Cdh8* and *Cdh9* loss on synaptic function, we recorded from ooDSGCs in the Hb9-GFP and TWY9-YFP lines while stimulating BC2s or BC5s optogenetically. The incidence of functional connections between BC2s and ooDSGCs was reduced from 53% to 11% in *cdh8* mutants compared to controls, while the average amplitude and latency in connected pairs was not significantly affected (Figure 4J). Likewise, the incidence but not the strength of connections between BC5s and ooDSGCs was significantly reduced in *cdh9* mutants (Figure 4K). These results suggest that cadherins promote connectivity of BC2s and BC5s to ooDSGCs. Surprisingly, the functional defects in both mutants are substantially more severe than expected from structural defects, raising the possibility that cadherins play distinct roles in arbor localization and synapse formation (see Discussion).

Cdh8 Is Required for Initial Targeting of BC Arbors

Cdh8 and *Cdh9* might regulate BC arborization by directing axonal targeting, refining initially diffuse arbors (Morgan et al., 2006), or maintaining lamina-restricted arbors once they have formed. To distinguish these alternatives, we analyzed control and mutant BC2s between P4 and P30 (Figures 4L–4S). We immunostained LacZ in the *Cdh8*^{LacZ} allele to visualize BCs,

because expression of Cre from the *Neto1*^{Cre} allele is undetectable until the second postnatal week. We attempted to perform similar studies with the *Cdh9*^{LacZ} allele, but levels of LacZ were too low to permit visualization of arbors.

Most BCs undergo their terminal division between birth and P5 (Morrow et al., 2008; Voinescu et al., 2009). LacZ was undetectable in the inner nuclear layer of *Cdh8*^{LacZ/+} and *Cdh8*^{LacZ/LacZ} mice prior to P4, suggesting that *cdh8* is not expressed in progenitors. LacZ was detectable by P6, as axons of BC2s reach the IPL. By this time, control axons were largely confined to the appropriate sublamina, whereas mutant axons extended into the inner portion of the IPL (Figures 4L and 4M). Aberrant projections accumulated over the subsequent week (Figures 4N–4S). By P21, defects assayed by LacZ expression were indistinguishable from those assayed by GFP expression (Figures 4B, 4D, and 4R–4T). These results suggest that *Cdh8* directs targeting of BC2 arbors.

Cdh8 and Cdh9 Act Instructively to Target BC Axons

Results presented so far are consistent with either a permissive or an instructive role for *Cdh8* and *Cdh9* in axonal arborization: BCs might require a cadherin to enact their developmental program, with specificity imparted by other molecules, or cadherins might provide positional information. To distinguish these alternatives, we overexpressed recombinant *Cdh8*- and *Cdh9*-mCherry fusion proteins in BCs by electroporation of Cre-dependent vectors. Both proteins mediated homophilic adhesion in heterologous cells (data not shown). Expression of *Cdh8*-mCherry in BC2s had no detectable effect on the arbors of these cells (Figures 3C, 5A, and 5B). In contrast, expression of *Cdh9*-mCherry led to displacement of their arbors to a position roughly corresponding to that of control BC5s (Figures 5C and 5D). Similarly, expression of *Cdh8*-mCherry, but not *Cdh9*-mCherry, displaced BC5 arbors to a position roughly corresponding to that of control BC2s (Figures 5D–5H). Displacement was not accompanied by a change in identity: OFF BC2s and ON BC5s remained negative and positive, respectively, for Islet1, an ON BC marker (Elshatory et al., 2007), whether or not their arbors were displaced (Figures S5S–S5V). Thus, cadherins exert differential effects on arbors of BCs.

As a critical test of the idea that type II cadherins play an instructive role, we introduced the *Cdh8*- and *Cdh9*-mCherry fusion proteins into a neuronal subtype that normally expresses neither *cdh8* nor *cdh9*. We chose a pair of closely related narrow-field amacrine subtypes called nGnG and SEG, both of which

(E–H) BC5s labeled in *Kcng4*^{Cre/+} (E), *Kcng4*^{Cre/+}; *Cdh8*^{LacZ/LacZ} (F), or *Kcng4*^{Cre/+}; *Cdh9*^{LacZ/LacZ} mice (G). (H) Mean intensity (\pm SEM) of YFP label across the IPL from images such as those shown in (E–G). n = 37 (E), n = 41 (F), and n = 44 (G). Sections in (A)–(C) and (E)–(G) were counterstained with Neurotrace (blue) and anti-VACHT (red). Scale bar represents 10 μ m.

(I) Axonal arbor centroid positions of individual BC2s and BC5s along the depth of the IPL. Arrows show centroid positions of OFF SAC, bistratified ooDSGC, and ON SAC dendrites (30%–35%, 45%–50%, and 60%–65% respectively).

(J) Currents recorded from ooDSGCs following two-photon stimulation of ChR2-YFP-positive BC2s in controls (black) or *cdh8* mutants (red). Graphs next to the traces show average peak amplitude of currents and fraction of pairs connected (n = 4 ooDSGCs with 472 BCs in controls and 6 ooDSGCs with 574 BCs in mutants). *p < 0.05.

(K) Currents recorded from ooDSGCs following two-photon stimulation of BC5s in controls (gray) or *cdh9* mutants (blue). Graphs next to the traces show average peak amplitude of currents and fraction of pairs connected (5 ooDSGCs with 422 BCs in controls and 6 ooDSGCs with 630 BCs in mutants). *p < 0.05.

(L–T) BC2s labeled with anti-LacZ in *Cdh8*^{LacZ/+} and *Cdh8*^{LacZ/LacZ} mice at P6 (L and M), P9 (N and O), P12 (P and Q), and P21 (R and S). Neurotrace (blue) and anti-VACHT (red). Scale bars represent 10 μ m. (T) Mean density (\pm SEM) of YFP label across the IPL from images such as those shown in (G) and (H). n = 15 (R) and 13 (S) Differences between mutants and controls in (D), (H), and (T). p < 10⁻⁵ by Chi-square test.

See also Figures S4 and S5 and Table S5.

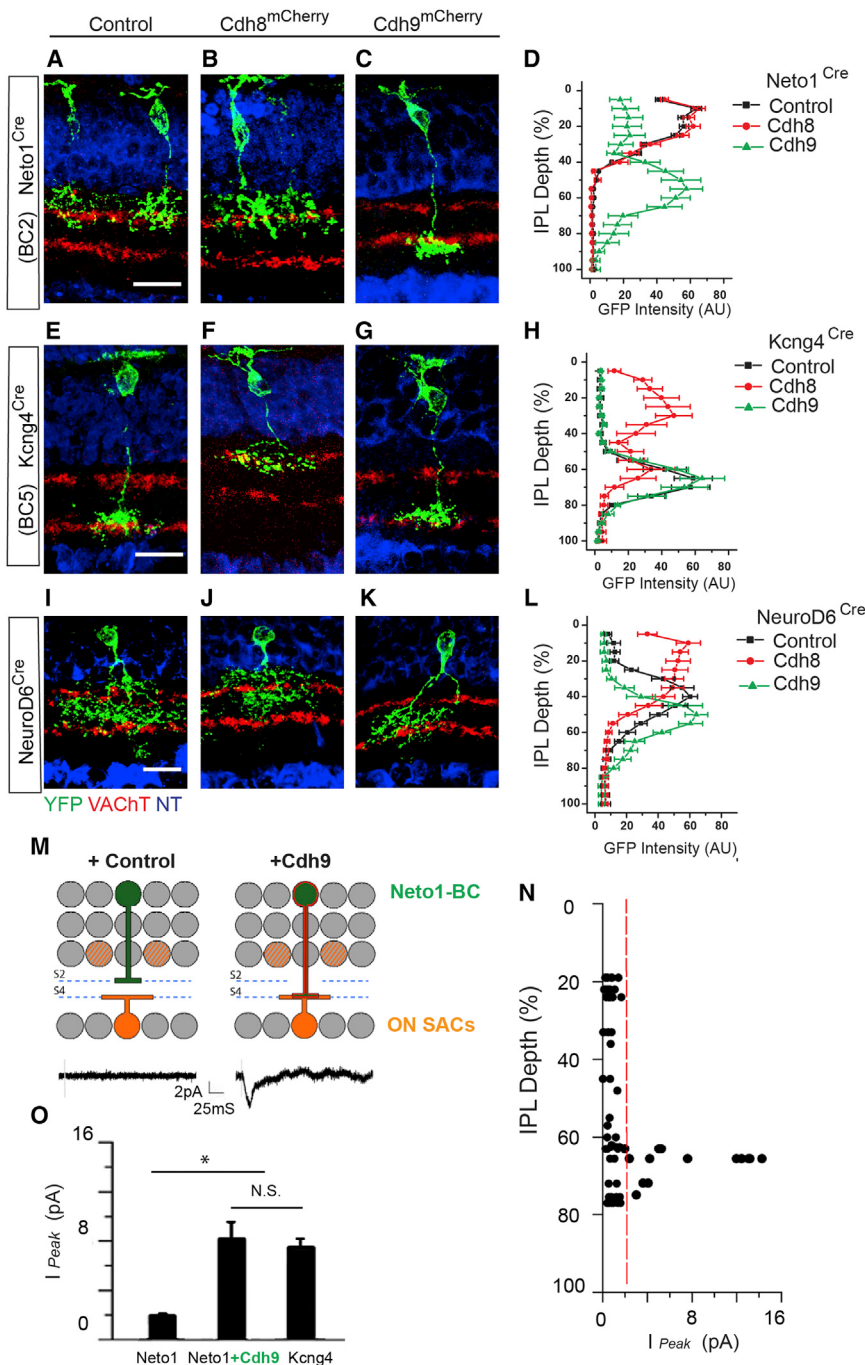


Figure 5. Ectopic Expression of Cdh8 and Cdh9 Reorients BC and AC Arbors

(A–D) BC2s labeled in *Neto1*^{Cre/+} mice electroporated with YFP alone (A), or with *Cdh8*-mCherry (B) or *Cdh9*-mCherry (C).

(E–H) BC5s labeled in *Kcng4*^{Cre/+} mice electroporated with YFP alone (E), or with *Cdh8*-mCherry (F) or *Cdh9*-mCherry (G).

(I–L) nGnG and SEG ACs labeled in *NeuroD6*^{Cre/+} electroporated with YFP alone (I), or with *Cdh8*-mCherry (J) or *Cdh9*-mCherry (K). Sections counterstained with Neurotrace (blue) and anti-VACHT (red). Scale bar represents 10 μ m. (D, H, and L) Mean intensity (\pm SEM) of YFP label across the IPL from images such as those shown in (A)–(C), (E)–(G), and (I)–(K). n = 35–45 per condition. Differences between mutants and controls, $p < 10^{-5}$ by Chi-square test.

(M) Currents recorded from ON SACs in response to two-photon stimulation of BC2s transduced with ChR2-YFP alone (left) with *Cdh9*-mCherry (right).

(N) Average peak amplitudes for ChR2-YFP plus *Cdh9*-mCherry transduced BC2s versus BC axonal position in the IPL. Amplitudes are from a 30 ms window following two-photon excitation (n = 46 pairs). The dotted line indicates the mean noise level as judged from stimulation of BC2s transduced with ChR2-YFP only. Only BC2s whose axons occupied a depth corresponding to the ON-SAC lamina produced currents two SD above the mean noise level.

(O) Average peak amplitudes measured on ON-SACs in response to two-photon stimulation from control BC2s, “connected” *Cdh9*-transduced BC2s and control BC5s (n = 7 ON-SACs and 884 BC2s for control amplitude. n = 5 ON-SACs and n = 14 “connected” *Cdh9*-transduced BC2s; BC5 to ON-SAC amplitudes are from Figures 2C and 2E. N.S.: $p > 0.05$, * $p < 0.05$.

See also Figures S5 and S6.

stratum in which BC5s arborize (Figures 5J–L and S6A–S6C). Thus, *Cdh8* and *Cdh9* are sufficient to instruct placement of arbors within the IPL.

Displaced Bipolar Arbors Form Functional Synapses

We asked whether BC2s form functional synapses with ON SACs when their arbors are displaced by ectopic expression

of *cdh9*. We electroporated ChR2-YFP or ChR2-YFP plus *Cdh9*-mCherry into BC2s of *Neto1*^{Cre/+}; Thy1-OFP3 mice, in which SACs were OFP-positive (Figures 5M and S6). As expected, arbors of most BC2s were displaced to the ON sublaminae. We recorded currents in ON SACs while imaging BC2 arbors with two-photon optics and stimulating them optogenetically (Figure S6). Stimulation of displaced, but not control, BC2s evoked currents in ON SACs (Figures 5M–O). The size and latency of currents from displaced BCs were similar to those evoked by BC5s in wild-type

express *NeuroD6* (Kay et al., 2011b). We used a *NeuroD6*^{Cre} line to manipulate these cells. Labeling with mCherry alone confirmed that the arbors of nGnG and SEG amacrine cells span the top two-thirds of the IPL with a center of mass that lies between the sublaminae in which BC2s and BC5s arborize (Figure 5I). Introduction of *Cdh8*-mCherry displaced arbors toward the outer portion of the IPL, closer to the stratum in which BC2s arborize, whereas introduction of *Cdh9*-mCherry displaced arbors toward the inner portion of the IPL, closer to the

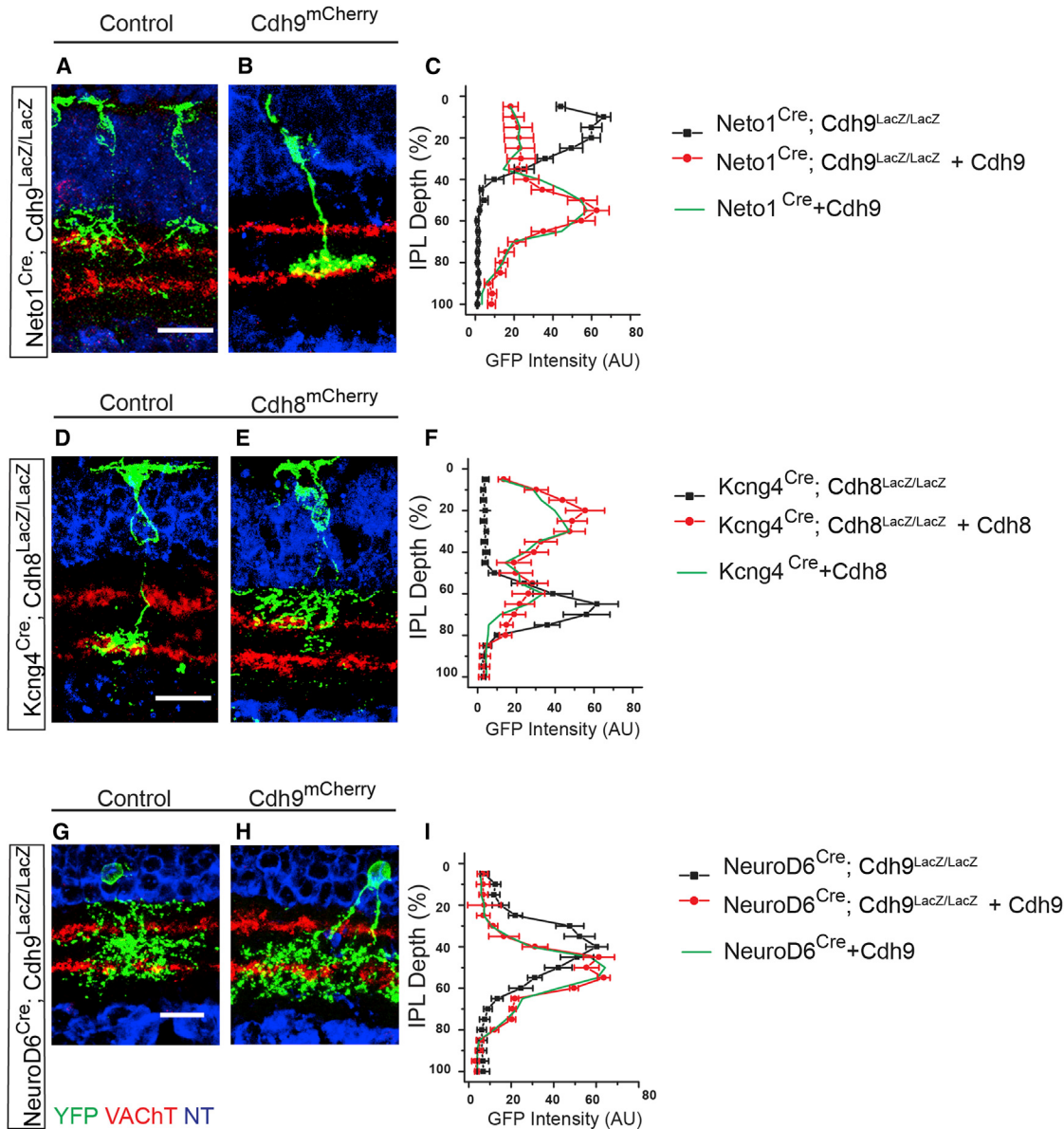


Figure 6. Cdh8 and Cdh9 Affect Arbor Position by a Heterophilic Mechanism

(A–C) BC2s labeled in *Neto1*^{Cre/+}; *Cdh9*^{LacZ/LacZ} mice electroporated with YFP alone (A), with *Cdh9*-mCherry (B).

(D–F) BC5s labeled in *Kcng4*^{Cre/+}; *Cdh8*^{LacZ/LacZ} mice electroporated with YFP alone (D), with *Cdh8*-mCherry (E).

(G–I) nGnG and SEG ACs labeled in *NeuroD6*^{Cre/+}; *Cdh9*^{LacZ/LacZ} mice electroporated with YFP alone (G), with *Cdh9*-mCherry (H). Sections counterstained with Neurotrace (blue) and anti-VAcT (red).

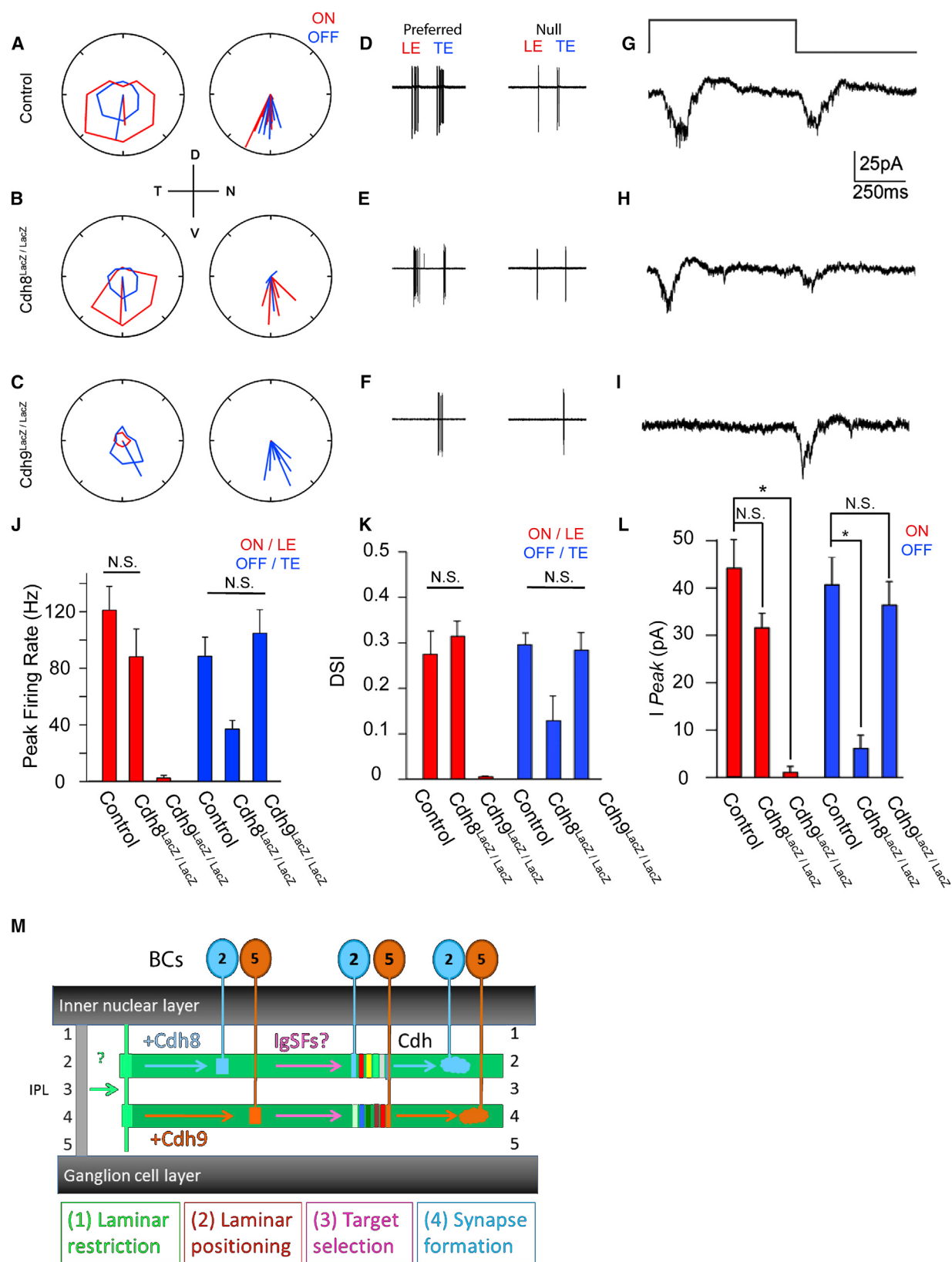
Scale bars represent 10 μ m. (C, F, and I) Mean intensity (\pm SEM) of YFP label across the IPL from images such as those shown in (A), (B), (D), (E), (G), and (H) ($n = 27$ –48 per condition). Control data from Figures 5D, 5H, and 5L are replotted without error bars.

animals (Figure 5O). Thus, redirected OFF BCs can form functional, ectopic synapses on postsynaptic cells in the ON pathway.

Cdh8 and Cdh9 Act Heterophilically

Classical cadherins are homophilic adhesion molecules (Hirano and Takeichi, 2012), so we reasoned that Cdh8 and Cdh9 on BCs might interact with Cdh8 and Cdh9 on neighboring BCs or on target cells.

To test this idea, we introduced Cdh8- or Cdh9-mCherry into small numbers of cells in *cdh8* or *cdh9* mutant backgrounds. In these mice, individual cells expressing ectopic cadherin did not encounter cells expressing that cadherin. We performed three sets of experiments: introduction of Cdh9-mCherry into BC2s in *cdh9* mutants, introduction of Cdh8-mCherry into BC5s in *cdh8* mutants, and introduction of Cdh9-mCherry into nGnG and SEG amacrine cells in *cdh9* mutants (Figures 6A–6I). In each of



(legend on next page)

three cases, laminar patterns of arbors in transduced mutants were indistinguishable from those in wild-type animals (Figures 6B, 6E, and 6H compared to Figures 5C, 5F, and 5K), providing strong evidence that Cdh8 and Cdh9 affect arborization of BC axons by a heterophilic rather than a homophilic mechanism.

Visual Responses of ooDSGCs Are Compromised in the Absence of Cdh8 or Cdh9

To ask how loss of Cdh8 or Cdh9 affects visual responses of ooDSGCs, we measured action potentials in ooDSGCs in response to bright bars passed in each of 8 directions (Figure 7A). By recording from ooDSGCs normally selective for ventral motion (Hb9-GFP), we could assess not only whether the responses were direction-selective but also whether loss of cadherins affected the preferred direction. As expected, control ooDSGCs responded vigorously both when a bright bar moving ventrally on a dark background entered the receptive field (ON response) and when it exited the field (OFF response); bars moving in other directions elicited weaker responses (Figures 7A and 7D).

Deletion of *cdh8* selectively decreased the OFF responses of the ooDSGC by ~60% compared to controls, whereas ON responses were preserved (Figures 7B, 7E, 7J, and S7B). Moreover, whereas the direction-selectivity of the residual OFF responses was reduced in *cdh8* mutants, that of the ON responses was unaffected (Figures 7B, 7E, and 7K). Conversely, in *cdh9* mutants, OFF responses were preserved and directional, but ON responses were nearly absent (Figures 7C, 7F, 7J, 7K and S7C).

The most likely explanation of these defects was a loss of excitatory currents from BCs to ooDSGCs, but it was also possible that altered inhibition played a role. To distinguish these alternatives, we recorded currents from ooDSGCs in response to moving bars and full field flashes (Figure 7G). Excitatory OFF currents were decreased while ON currents were unaffected in *cdh8* mutants, whereas excitatory ON currents were selectively lost in *cdh9* mutants (Figures 7H, 7I, and 7L). Thus, ooDSGCs generalize about direction of motion by summing independent inputs from Cdh9-dependent ON and Cdh8-dependent OFF channels (Kittila and Massey, 1995).

DISCUSSION

Processes of ~100 neuronal subtypes intermingle in the restricted confines of the developing IPL. During the first few

postnatal weeks, they form the specific patterns of synaptic connectivity that enable sophisticated processing of visual information. Although electrical activity or visual experience can affect synapse number, it has little effect on laminar restriction of arbors and synapses (Kerschensteiner et al., 2009; Wei and Feller, 2011). Thus, it is likely that patterns of connectivity are molecularly specified in these circuits. Here, we show that BC2s and BC5s deliver visual input to neurons that compute direction of motion and demonstrate that Cdh8 and Cdh9 are required for assembly of the circuit.

Genetic Access to Neural Circuits

Our approach required gaining genetic access to the neuron types that comprise the ON-OFF direction-selective circuit. It is a major advantage of the retina for circuit analysis that many of its neuronal subtypes have been characterized morphologically, physiologically and molecularly. For many other parts of the CNS, analysis of how specific connections form as circuits assemble is not yet feasible. We used eight genetically engineered lines that allowed us to mark and manipulate six neuronal types in this circuit (Figure 1B): two types of BCs (BC2s and BC5s), two types of amacrine cells (ON and OFF SACs), and two types of ooDSGCs (preferring ventral or temporal motion).

Connections between SACs and ooDSGCs had been described previously (Briggman et al., 2011; Fried et al., 2002), but it was unclear which BC types transfer visual input from photoreceptors to SACs and ooDSGCs. Our optogenetic analysis provided direct evidence that BC2s and BC5s synapse on SACs and ooDSGCs. Results of a recent electron microscopy study are consistent with this conclusion, with the caveat that the method used scored contacts rather than ultrastructurally specialized synapses (Helmstaedter et al., 2013). In addition, Yonehara et al. (2013) recently demonstrated connections of BC5s with ON-DSGCs, whose dendrites costratify with ooDSGCs. It remains to be determined whether other BC types also form synapses on SACs and ooDSGCs. Our functional studies (Figure 7) suggest that BC5s provide the major ON inputs to ooDSGCs but that BCs other than BC2s provide OFF input.

Instructive Role for Type II Cadherins

The cadherin superfamily comprises >100 cell surface glycoproteins defined by the presence of conserved extracellular domains. The first three cadherins to be identified (Cdh1–Cdh3)

Figure 7. Removal of Cdh8 and Cdh9 Abolish ON and OFF Channels on ooDSGCs

- (A–C) Polar plots for firing rates and direction-selectivity index (DSI) from sample ooDSGCs (left) and DSI of the full population of ooDSGCs (right) in controls (A), *cdh8* mutants (B) and *cdh9* mutants(C) in response to a bright bar moving in eight different directions ($n = 9$ Hb9GFP ooDSGCs in controls; $n = 6$ in *Cdh8^{LacZ/LacZ}*; $n = 7$ in *Cdh9^{LacZ/LacZ}*). Radius = 120 Hz in left panels and 0.5 in right panels.
- (D–F) Sample leading edge (LE, ON) and trailing edge (TE, OFF) responses to a bright bar moving in the preferred and null directions.
- (G–I) Sample whole-cell currents measured on HB9-GFP ooDSGCs in controls (G), *cdh8* mutants (H), and *cdh9* mutants (I) at $V_h = -60$ mV in response to a flashing spot (about 200 μ m) centered on the receptive field. OFF and ON responses were dramatically reduced in *cdh8* and *cdh9* mutants, respectively.
- (J) Average peak action potential firing rates for the leading edge and trailing edge of a bar moving in the preferred direction on HB9-GFP ooDSGCs in (D)–(F). $n = 9$ for controls; $n = 6$ for *Cdh8^{LacZ/LacZ}*; $n = 7$ for *Cdh9^{LacZ/LacZ}*. N.S.: $p > 0.05$.
- (K) Average direction selectivity index (DSI) computed from population vectors in (A)–(C). $n = 9$ for controls; $n = 6$ for *Cdh8^{LacZ/LacZ}*, $n = 7$ for *Cdh9^{LacZ/LacZ}*. N.S.: $p > 0.05$.
- (L) Average peak light-evoked current amplitude to ON and OFF transitions in spot intensity for HB9-GFP ooDSGCs in controls, *cdh8* and *cdh9* mutants shown in (G)–(I). $n = 7$ for each condition; N.S.: $p > 0.05$, * $p < 0.05$.
- (M) A model for selective synapse formation by bipolar cells in retina (see Discussion).

See also Figure S7.

and their closest relatives are now classified as classical cadherins, which are in turn divided into type I (*Cdh1–Cdh4* and *Cdh15*) and type II (*Cdh5–Cdh12*, *Cdh18–Cdh20*, *Cdh22*, and *Cdh24*). They play critical roles in development and maintenance of tissues throughout the vertebrate body (Lien et al., 2006). In the nervous system, they have been implicated in numerous developmental events, including neurulation, neuronal migration, aggregation of neurons into nuclei and pools, neurite growth, axonal fasciculation, synaptic differentiation, and plasticity (Inoue and Sanes, 1997; Osterhout et al., 2011; Paradis et al., 2007; Price et al., 2002; Suzuki et al., 2007; Tanabe et al., 2006; Tang et al., 1998; Williams et al., 2011; reviewed in Hirano and Takeichi, 2012).

Classical cadherins exhibit complex, dynamic, and combinatorial patterns of expression in many parts of developing and adult CNS (Krishna-K et al., 2011; Redies, 2000) including the retina (Etzrodt et al., 2009; Honjo et al., 2000; Wöhrn et al., 1998; Yamagata et al., 2006). These patterns led to the idea that cadherins comprise an “adhesive code” underlying specific connectivity among neurons or regions (Redies and Takeichi, 1996). To date, however, support for this hypothesis has been limited (Hirano and Takeichi, 2012). Indeed, cadherin appears to mediate selective connectivity by spatiotemporally regulated expression rather than adhesive diversity in *Drosophila* (Nern et al., 2008).

Our results provide strong support for the hypothesis that cadherins do, in fact, comprise components of an “adhesive code.” Initial evidence came from the altered BC arbors observed in the absence of *Cdh8* and *Cdh9*. These results were compatible with either permissive or instructive roles. For example, each BC subtype could require a cadherin to form a suitable arbor, with the site of the arbor determined by other molecules. Alternatively, *Cdh8* and *Cdh9* could be specific determinants of arbor position. Gain-of-function experiments allowed us to distinguish between these models: introduction of *Cdh8* and *Cdh9* had distinct effects on arbors of BC2s and BC5s, as well as amacrine cells that normally expressed neither. Together, these results demonstrate that *Cdh8* and *Cdh9* play instructive rather than (or in addition to; see below) permissive roles in circuit assembly. Moreover, the roles are specific: of the many cell types we analyzed, *Cdh8* and *Cdh9* organized target choices of only BC2s and BC5s.

Type II cadherins may play related roles in other parts of the CNS. For example, the efficacy of connections between a population of thermosensitive neurons and their targets in the spinal cord is reduced in *cdh8* mutants (Suzuki et al., 2007) and knockdown of *Cdh9* decreases synaptic transmission from dentate granule cells to CA3 neurons in the hippocampus (Williams et al., 2011). Instructive roles of cadherins were not, however, sought in these studies. In addition, microdeletions in *cdh8* and polymorphisms near the *cdh9* locus have been detected in rare autistic individuals (Pagnamenta et al., 2011; Wang et al., 2009). Defects in cortical circuitry have been hypothesized to underlie symptoms of autism.

Ligands of Cadherins

Homophilic adhesion has been demonstrated for numerous classical cadherins and protocadherins, and this adhesion is generally believed to underlie their function (Brasch et al.,

2012; Schreiner and Weiner, 2010). Yet, two lines of evidence indicate that *Cdh8* and *Cdh9* act heterophilically in the retina. First, we could not detect *Cdh8* or *Cdh9* in neighboring cells during the synaptogenesis of BCs. Second, ectopic expression of *cdh8* or *cdh9* redirected axons of individual neurons in mutant mice in which neighboring neurons lacked the cognate cadherin.

How then might these cadherins act? We consider three possibilities. First, *Cdh8* and *Cdh9* might bind to noncadherin ligands on neighboring cells. To date, however, no such ligands have been described. Second, cadherins bind in *cis* to other adhesive proteins such as nectins and nonclustered protocadherins, and this interaction can affect the binding specificity of both the cadherin and its partner (Biswas et al., 2010; Morita et al., 2010). Such partners could interact differentially with *Cdh8* and *Cdh9* in *cis* and with other ligands on neighboring cells. Third, *Cdh8* and *Cdh9* could interact with other cadherins. Indeed, some cadherins have been shown to bind heterophilically to closely related family members in heterologous cells (Shimoyama et al., 2000). In particular, *Cdh8* binds to *Cdh11*, while *Cdh9* binds to *Cdh6* and *Cdh10* (Shimoyama et al., 2000). Interestingly, SACs and some oodSGCs express *cdh6* (Kay et al., 2011a). Analysis of double and triple mutants could reveal roles masked by compensation or redundancy in single mutants.

Model of Synaptic Choice in Retina

We conclude with a speculative, but testable, model for roles of *Cdh8* and *Cdh9* in retinal circuit assembly. First, we suggest that a prepattern in the IPL renders two strata potentially attractive to both BC2s and BC5s (Figure 7M, Step 1). This is because deletion of *cdh8* redistributes the arbors of BC2s such that about half remain in their proper sublamina whereas the other half are displaced to the sublamina in which BC5s normally arborize; deletion of *cdh9* has a similar, albeit less striking, effect on BC5s. In this scheme, the role of cadherins is not to precisely specify the position of BC axonal arbors but rather to bias their choice between the two potential sublaminae (Figure 7M, Step 2). Evidence for this step is that introduction of *Cdh8* at high levels leads to a dramatic shift of arbors from ON to OFF sublamina and vice versa for *Cdh9*. A prediction of this model is that ligands capable of distinguishing between *Cdh8* and *Cdh9* are localized to these sublaminae.

Intriguingly the cadherin-dependent choice appears to be between positions that are symmetrically displaced from the midline of the IPL. In fact, there is considerable evidence for the presence of “paramorphic pairs” of ON and OFF RGC that are similar in morphology except for symmetrical displacement of their arbors (Coombs et al., 2006; Hong et al., 2011). Likewise, ON and OFF SACs can be viewed as a paramorphic pair. Of particular interest is the finding that dendrites of two OFF subtypes were displaced to a corresponding position in the ON region of the IPL in *sema6A* and *plexA4* mutants (Matsuoka et al., 2011). A design principle of retinal circuit assembly could thus be a stepwise division of the IPL into mirror-symmetric sets of ON and OFF domains followed by assignment of paramorphic pairs to one or the other.

Once in the proper sublamina, BC axons choose among dendrites of multiple amacrine and ganglion cells (Figure 7M,

Step 3). Cadherins might mediate this step as well, but it is unlikely that a single recognition molecule will be sufficient to explain the complex patterns of connectivity exhibited by any retinal neuron. Moreover, immunoglobulin superfamily molecules such as Sidekicks (Yamagata and Sanes, 2008, 2012) are capable of mediating intralaminar choice (A.K., M. Yamagata, X.D., and J.R.S., unpublished data). Thus, it is attractive to posit a combinatorial model in which multiple adhesion molecules collaborate to ensure specific connectivity.

Finally, once synaptic contacts are established, they become functional (Figure 7M, Step 4). Surprisingly, the physiological defects detected in the cadherin mutants were significantly greater than those predicted from the morphological defects. That is, most axons of *cdh8* mutant BC2s and *cdh9* mutant BC5s were in close proximity to the dendrites of ooDSGCs, yet transmission from BCs to ooDSGCs was reduced by ~80% (Figure 4). Although ultrastructural studies will be needed to assess the extent of this proximity, we suggest that cadherins play not only an instructive role in specifying synaptic location, but also a permissive role in synapse formation. In this model, Cdh8 and Cdh9 provide distinct information about location and targets but a variety of cadherins could suffice to enable transmission. Rescue of the mutants by introduction of chimeric cadherins using the methods shown in Figure 5 could provide a way to test this idea.

EXPERIMENTAL PROCEDURES

Animals

Cre recombinase was inserted into the translation start codon of the *neto1* and *kcnq4* genes by homologous recombination, generating *Neto1^{Cre}* and *Kcnq4^{Cre}* lines. *Cdh9^{LacZ}* mice were produced as described in the [Extended Experimental Procedures](#), generating a null allele. Other lines have been described previously: ChAT^{Cre} (Rossi et al., 2011), TYW9-YFP (Kim et al., 2010), *Cdh8^{LacZ}* (Suzuki et al., 2007), Thy1-stop-YFP Line#1 (Buffelli et al., 2003), HB9-GFP (Trenholm et al., 2011), RC-stop-ChR2-Tdtomato (Ai27) (Madsen et al., 2012), and Thy1-OFP3 (Kay et al., 2012). Animals were used in accordance with NIH guidelines and protocols approved by Institutional Animal Use and Care Committee at Harvard University.

Gene Transfer

Retinal cells were transduced *in vivo* by electroporation of purified DNA as described by Matsuda and Cepko (2007) or adeno-associated viral vectors (Hong et al., 2011).

Electrophysiology

Mice were dark adapted for at least 2 hr prior to euthanasia. The retina was rapidly dissected under infrared illumination and the retina was placed in a recording chamber on the stage of a custom built two-photon microscope. Fluorescent cells were imaged and targeted for recording with patch electrodes. Neurons were imaged and optogenetically stimulated using a custom-built two-photon microscope, and currents or spikes were recorded in whole-cell or loose-patch modes. Channelrhodopsin was excited using two-photon excitation to avoid stimulation of photoreceptors. Light stimuli were delivered from a projector with a custom substage lens system focused onto the photoreceptors.

Histology

Retinas were analyzed as whole mounts or cryosections as described by Kim et al. (2010). *In situ* hybridization was performed as described by Kay et al. (2011a).

Further descriptions of histological, molecular, physiological, and imaging methods are provided in the [Extended Experimental Procedures](#).

SUPPLEMENTAL INFORMATION

Supplemental Information includes Extended Experimental Procedures, seven figures, and five tables and can be found with this article online at <http://dx.doi.org/10.1016/j.cell.2014.06.047>.

AUTHOR CONTRIBUTIONS

X.D., A.K., and J.R.S planned experiments, analyzed data, and wrote the paper. X.D. conducted genetic, molecular, and imaging experiments. A.K. designed and built the optogenetic and recording apparatus and conducted electrophysiological and imaging experiments. I.D.I.H. performed the *in situ* hybridization screen.

ACKNOWLEDGMENTS

We thank M. Takeichi for *Cdh8^{LacZ}* mice, H. Zeng for Ai27 mice; P. Arlotta for 5HT3R-GFP mice; M. Williams for the *cdh9* cDNA; M. Yamagata, I-J. Kim, J. Kay, E. Soucy, and J. Greenwood for advice and assistance; J. Johnson (Penn Vector Core) for advice on AAV serotypes; and the Genome Modification Facility (GMF) at Harvard for generating mouse lines. This work was supported by grants from NIH (NS029169 and EY022073 to J.R.S.), a Natural Sciences and Engineering Research Council (NSERC) Fellowship to I.D.I.H., NSERC and Banting Fellowships to A.K., and a Howard Hughes Medical Institute-Life Sciences Research Foundation (HHMI-LSRF) Fellowship to X.D.

Received: March 1, 2014

Revised: May 10, 2014

Accepted: June 20, 2014

Published: August 14, 2014

REFERENCES

- Andrasfalvy, B.K., Zemelman, B.V., Tang, J., and Vaziri, A. (2010). Two-photon single-cell optogenetic control of neuronal activity by sculpted light. *Proc. Natl. Acad. Sci. USA* 107, 11981–11986.
- Biswas, S., Emond, M.R., and Jontes, J.D. (2010). Protocadherin-19 and N-cadherin interact to control cell movements during anterior neurulation. *J. Cell Biol.* 191, 1029–1041.
- Brasch, J., Harrison, O.J., Honig, B., and Shapiro, L. (2012). Thinking outside the cell: how cadherins drive adhesion. *Trends Cell Biol.* 22, 299–310.
- Briggman, K.L., Helmstaedter, M., and Denk, W. (2011). Wiring specificity in the direction-selectivity circuit of the retina. *Nature* 471, 183–188.
- Buffelli, M., Burgess, R.W., Feng, G., Lobe, C.G., Lichtman, J.W., and Sanes, J.R. (2003). Genetic evidence that relative synaptic efficacy biases the outcome of synaptic competition. *Nature* 424, 430–434.
- Cardin, J.A., Carlén, M., Meletis, K., Knoblich, U., Zhang, F., Deisseroth, K., Tsai, L.H., and Moore, C.I. (2009). Driving fast-spiking cells induces gamma rhythm and controls sensory responses. *Nature* 459, 663–667.
- Chow, R.L., Volgyi, B., Szilard, R.K., Ng, D., McKerlie, C., Bloomfield, S.A., Birch, D.G., and McInnes, R.R. (2004). Control of late off-center cone bipolar cell differentiation and visual signaling by the homeobox gene *Vsx1*. *Proc. Natl. Acad. Sci. USA* 101, 1754–1759.
- Coombs, J., van der List, D., Wang, G.Y., and Chalupa, L.M. (2006). Morphological properties of mouse retinal ganglion cells. *Neuroscience* 140, 123–136.
- De la Huerta, I., Kim, I.J., Voinescu, P.E., and Sanes, J.R. (2012). Direction-selective retinal ganglion cells arise from molecularly specified multipotential progenitors. *Proc. Natl. Acad. Sci. USA* 109, 17663–17668.
- Elshatory, Y., Deng, M., Xie, X., and Gan, L. (2007). Expression of the LIM-homeodomain protein *Isl1* in the developing and mature mouse retina. *J. Comp. Neuro.* 503, 182–197.
- Etzrodt, J., Krishna-K, K., and Redies, C. (2009). Expression of classic cadherins and delta-protocadherins in the developing ferret retina. *BMC Neurosci.* 10, 153.

- Famiglietti, E.V., Jr., and Kolb, H. (1976). Structural basis for ON-and OFF-center responses in retinal ganglion cells. *Science* 194, 193–195.
- Fried, S.I., Münch, T.A., and Werblin, F.S. (2002). Mechanisms and circuitry underlying directional selectivity in the retina. *Nature* 420, 411–414.
- Gollisch, T., and Meister, M. (2010). Eye smarter than scientists believed: neural computations in circuits of the retina. *Neuron* 65, 150–164.
- Haverkamp, S., Ghosh, K.K., Hirano, A.A., and Wässle, H. (2003). Immunocytochemical description of five bipolar cell types of the mouse retina. *J. Comp. Neuro.* 455, 463–476.
- Haverkamp, S., Inta, D., Monyer, H., and Wässle, H. (2009). Expression analysis of green fluorescent protein in retinal neurons of four transgenic mouse lines. *Neuroscience* 160, 126–139.
- Helmaedter, M., Briggman, K.L., Turaga, S.C., Jain, V., Seung, H.S., and Denk, W. (2013). Connectomic reconstruction of the inner plexiform layer in the mouse retina. *Nature* 500, 168–174.
- Hirano, S., and Takeichi, M. (2012). Cadherins in brain morphogenesis and wiring. *Physiol. Rev.* 92, 597–634.
- Hong, Y.K., Kim, I.J., and Sanes, J.R. (2011). Stereotyped axonal arbors of retinal ganglion cell subsets in the mouse superior colliculus. *J. Comp. Neuro.* 519, 1691–1711.
- Honjo, M., Tanihara, H., Suzuki, S., Tanaka, T., Honda, Y., and Takeichi, M. (2000). Differential expression of cadherin adhesion receptors in neural retina of the postnatal mouse. *Invest. Ophthalmol. Vis. Sci.* 41, 546–551.
- Huberman, A.D., Wei, W., Elstrott, J., Stafford, B.K., Feller, M.B., and Barres, B.A. (2009). Genetic identification of an On-Off direction-selective retinal ganglion cell subtype reveals a layer-specific subcortical map of posterior motion. *Neuron* 62, 327–334.
- Inoue, A., and Sanes, J.R. (1997). Lamina-specific connectivity in the brain: regulation by N-cadherin, neurotrophins, and glycoconjugates. *Science* 276, 1428–1431.
- Kay, J.N., De la Huerta, I., Kim, I.J., Zhang, Y., Yamagata, M., Chu, M.W., Meister, M., and Sanes, J.R. (2011a). Retinal ganglion cells with distinct directional preferences differ in molecular identity, structure, and central projections. *J. Neurosci.* 31, 7753–7762.
- Kay, J.N., Voineskos, P.E., Chu, M.W., and Sanes, J.R. (2011b). Neurod6 expression defines new retinal amacrine cell subtypes and regulates their fate. *Nat. Neurosci.* 14, 965–972.
- Kay, J.N., Chu, M.W., and Sanes, J.R. (2012). MEGF10 and MEGF11 mediate homotypic interactions required for mosaic spacing of retinal neurons. *Nature* 483, 465–469.
- Kerschensteiner, D., Morgan, J.L., Parker, E.D., Lewis, R.M., and Wong, R.O. (2009). Neurotransmission selectively regulates synapse formation in parallel circuits *in vivo*. *Nature* 460, 1016–1020.
- Kim, D.S., Ross, S.E., Trimarchi, J.M., Aach, J., Greenberg, M.E., and Cepko, C.L. (2008). Identification of molecular markers of bipolar cells in the murine retina. *J. Comp. Neuro.* 507, 1795–1810.
- Kim, I.J., Zhang, Y., Meister, M., and Sanes, J.R. (2010). Laminar restriction of retinal ganglion cell dendrites and axons: subtype-specific developmental patterns revealed with transgenic markers. *J. Neurosci.* 30, 1452–1462.
- Kittila, C.A., and Massey, S.C. (1995). Effect of ON pathway blockade on directional selectivity in the rabbit retina. *J. Neurophysiol.* 73, 703–712.
- Krishna-K, K., Hertel, N., and Redies, C. (2011). Cadherin expression in the somatosensory cortex: evidence for a combinatorial molecular code at the single-cell level. *Neuroscience* 175, 37–48.
- Lefebvre, J.L., Kostadinov, D., Chen, W.V., Maniatis, T., and Sanes, J.R. (2012). Protocadherins mediate dendritic self-avoidance in the mammalian nervous system. *Nature* 488, 517–521.
- Lien, W.H., Klezovitch, O., and Vasioukhin, V. (2006). Cadherin-catenin proteins in vertebrate development. *Curr. Opin. Cell Biol.* 18, 499–506.
- Madisen, L., Mao, T., Koch, H., Zhuo, J.M., Berenyi, A., Fujisawa, S., Hsu, Y.W., Garcia, A.J., 3rd, Gu, X., Zanella, S., et al. (2012). A toolbox of Cre-dependent optogenetic transgenic mice for light-induced activation and silencing. *Nat. Neurosci.* 15, 793–802.
- Masland, R.H. (2012). The neuronal organization of the retina. *Neuron* 76, 266–280.
- Matsuda, T., and Cepko, C.L. (2007). Controlled expression of transgenes introduced by *in vivo* electroporation. *Proc. Natl. Acad. Sci. USA* 104, 1027–1032.
- Matsuoka, R.L., Nguyen-Ba-Charvet, K.T., Parry, A., Badea, T.C., Chédotal, A., and Kolodkin, A.L. (2011). Transmembrane semaphorin signalling controls laminar stratification in the mammalian retina. *Nature* 470, 259–263.
- Morgan, J.L., Dhingra, A., Vardi, N., and Wong, R.O. (2006). Axons and dendrites originate from neuroepithelial-like processes of retinal bipolar cells. *Nat. Neurosci.* 9, 85–92.
- Morita, H., Nandadasa, S., Yamamoto, T.S., Terasaka-Iioka, C., Wylie, C., and Ueno, N. (2010). Nectin-2 and N-cadherin interact through extracellular domains and induce apical accumulation of F-actin in apical constriction of Xenopus neural tube morphogenesis. *Development* 137, 1315–1325.
- Morrow, E.M., Chen, C.M., and Cepko, C.L. (2008). Temporal order of bipolar cell genesis in the neural retina. *Neural Dev.* 3, 2.
- Nern, A., Zhu, Y., and Zipursky, S.L. (2008). Local N-cadherin interactions mediate distinct steps in the targeting of lamina neurons. *Neuron* 58, 34–41.
- Osterhout, J.A., Josten, N., Yamada, J., Pan, F., Wu, S.W., Nguyen, P.L., Panagiotaikos, G., Inoue, Y.U., Egusa, S.F., Volgyi, B., et al. (2011). Cadherin-6 mediates axon-target matching in a non-image-forming visual circuit. *Neuron* 71, 632–639.
- Oyster, C.W., and Barlow, H.B. (1967). Direction-selective units in rabbit retina: distribution of preferred directions. *Science* 155, 841–842.
- Pagnamenta, A.T., Khan, H., Walker, S., Gerrelli, D., Wing, K., Bonaglia, M.C., Giorda, R., Berney, T., Mani, E., Molteni, M., et al. (2011). Rare familial 16q21 microdeletions under a linkage peak implicate cadherin 8 (CDH8) in susceptibility to autism and learning disability. *J. Med. Genet.* 48, 48–54.
- Paradis, S., Harrar, D.B., Lin, Y., Koon, A.C., Hauser, J.L., Griffith, E.C., Zhu, L., Brass, L.F., Chen, C., and Greenberg, M.E. (2007). An RNAi-based approach identifies molecules required for glutamatergic and GABAergic synapse development. *Neuron* 53, 217–232.
- Price, S.R., De Marco Garcia, N.V., Ranscht, B., and Jessell, T.M. (2002). Regulation of motor neuron pool sorting by differential expression of type II cadherins. *Cell* 109, 205–216.
- Redies, C. (2000). Cadherins in the central nervous system. *Prog. Neurobiol.* 61, 611–648.
- Redies, C., and Takeichi, M. (1996). Cadherins in the developing central nervous system: an adhesive code for segmental and functional subdivisions. *Dev. Biol.* 180, 413–423.
- Rickgauer, J.P., and Tank, D.W. (2009). Two-photon excitation of channelrhodopsin-2 at saturation. *Proc. Natl. Acad. Sci. USA* 106, 15025–15030.
- Rossi, J., Balthasar, N., Olson, D., Scott, M., Berglund, E., Lee, C.E., Choi, M.J., Lauzon, D., Lovell, B.B., and Elmquist, J.K. (2011). Melanocortin-4 receptors expressed by cholinergic neurons regulate energy balance and glucose homeostasis. *Cell Metab.* 13, 195–204.
- Sanes, J.R., and Zipursky, S.L. (2010). Design principles of insect and vertebrate visual systems. *Neuron* 66, 15–36.
- Schreiner, D., and Weiner, J.A. (2010). Combinatorial homophilic interaction between gamma-protocadherin multimers greatly expands the molecular diversity of cell adhesion. *Proc. Natl. Acad. Sci. USA* 107, 14893–14898.
- Shimoyama, Y., Tsujimoto, G., Kitajima, M., and Natori, M. (2000). Identification of three human type-II classic cadherins and frequent heterophilic interactions between different subclasses of type-II classic cadherins. *Biochem. J.* 349, 159–167.
- Siebert, S., Scherf, B.G., Del Punta, K., Didkovsky, N., Heintz, N., and Roska, B. (2009). Genetic address book for retinal cell types. *Nat. Neurosci.* 12, 1197–1204.

- Sun, L.O., Jiang, Z., Rivlin-Etzion, M., Hand, R., Brady, C.M., Matsuoka, R.L., Yau, K.W., Feller, M.B., and Kolodkin, A.L. (2013). On and off retinal circuit assembly by divergent molecular mechanisms. *Science* 342, 1241974.
- Suzuki, S.C., Furue, H., Koga, K., Jiang, N., Nohmi, M., Shimazaki, Y., Katoh-Fukui, Y., Yokoyama, M., Yoshimura, M., and Takeichi, M. (2007). Cadherin-8 is required for the first relay synapses to receive functional inputs from primary sensory afferents for cold sensation. *J. Neurosci.* 27, 3466–3476.
- Tanabe, K., Takahashi, Y., Sato, Y., Kawakami, K., Takeichi, M., and Nakagawa, S. (2006). Cadherin is required for dendritic morphogenesis and synaptic terminal organization of retinal horizontal cells. *Development* 133, 4085–4096.
- Tang, L., Hung, C.P., and Schuman, E.M. (1998). A role for the cadherin family of cell adhesion molecules in hippocampal long-term potentiation. *Neuron* 20, 1165–1175.
- Trenholm, S., Johnson, K., Li, X., Smith, R.G., and Awatramani, G.B. (2011). Parallel mechanisms encode direction in the retina. *Neuron* 71, 683–694.
- Vaney, D.I., Sivyer, B., and Taylor, W.R. (2012). Direction selectivity in the retina: symmetry and asymmetry in structure and function. *Nat. Rev. Neurosci.* 13, 194–208.
- Voinescu, P.E., Kay, J.N., and Sanes, J.R. (2009). Birthdays of retinal amacrine cell subtypes are systematically related to their molecular identity and soma position. *J. Comp. Neuro.* 517, 737–750.
- Wang, K., Zhang, H., Ma, D., Bucan, M., Glessner, J.T., Abrahams, B.S., Salyakina, D., Imielinski, M., Bradfield, J.P., Sieiman, P.M., et al. (2009). Common genetic variants on 5p14.1 associate with autism spectrum disorders. *Nature* 459, 528–533.
- Wässle, H., Puller, C., Müller, F., and Haverkamp, S. (2009). Cone contacts, mosaics, and territories of bipolar cells in the mouse retina. *J. Neurosci.* 29, 106–117.
- Wei, W., and Feller, M.B. (2011). Organization and development of direction-selective circuits in the retina. *Trends Neurosci.* 34, 638–645.
- Williams, M.E., Wilke, S.A., Daggett, A., Davis, E., Otto, S., Ravi, D., Ripley, B., Bushong, E.A., Ellisman, M.H., Klein, G., and Ghosh, A. (2011). Cadherin-9 regulates synapse-specific differentiation in the developing hippocampus. *Neuron* 71, 640–655.
- Wöhrn, J.C., Puelles, L., Nakagawa, S., Takeichi, M., and Redies, C. (1998). Cadherin expression in the retina and retinofugal pathways of the chicken embryo. *J. Comp. Neurol.* 396, 20–38.
- Yamagata, M., and Sanes, J.R. (2008). Dscam and Sidekick proteins direct lamina-specific synaptic connections in vertebrate retina. *Nature* 451, 465–469.
- Yamagata, M., and Sanes, J.R. (2012). Expanding the Ig superfamily code for laminar specificity in retina: expression and role of contactins. *J. Neurosci.* 32, 14402–14414.
- Yamagata, M., Weiner, J.A., Dulac, C., Roth, K.A., and Sanes, J.R. (2006). Labeled lines in the retinotectal system: markers for retinorecipient sublaminae and the retinal ganglion cell subsets that innervate them. *Mol. Cell. Neurosci.* 33, 296–310.
- Yonehara, K., Farrow, K., Ghanem, A., Hillier, D., Balint, K., Teixeira, M., Jüttner, J., Noda, M., Neve, R.L., Conzelmann, K.K., and Roska, B. (2013). The first stage of cardinal direction selectivity is localized to the dendrites of retinal ganglion cells. *Neuron* 79, 1078–1085.